

Large-amplitude thermal oscillations in defected, tilted nanocolumns

Bradley C. Hubartt and Jacques G. Amar

Citation: [Applied Physics Letters](#) **105**, 193107 (2014); doi: 10.1063/1.4901741

View online: <http://dx.doi.org/10.1063/1.4901741>

View Table of Contents: <http://scitation.aip.org/content/aip/journal/apl/105/19?ver=pdfcov>

Published by the [AIP Publishing](#)

Articles you may be interested in

[Revealing the tunable twinning/detwinning behavior in 25nm Cu/Au multilayers](#)

Appl. Phys. Lett. **102**, 211905 (2013); 10.1063/1.4808036

[Microstructure and vacancy-type defects of high-pressure torsion deformed Al-3wt%Cu alloy](#)

J. Appl. Phys. **112**, 103506 (2012); 10.1063/1.4765034

[Superhard behaviour, low residual stress, and unique structure in diamond-like carbon films by simple bilayer approach](#)

J. Appl. Phys. **112**, 023518 (2012); 10.1063/1.4739287

[Correlation and size dependence of the lattice strain, binding energy, elastic modulus, and thermal stability for Au and Ag nanostructures](#)

J. Appl. Phys. **109**, 074319 (2011); 10.1063/1.3569743

[Radial compression studies of WS₂ nanotubes in the elastic regime](#)

J. Vac. Sci. Technol. B **29**, 021009 (2011); 10.1116/1.3549132

The advertisement features a dark blue background with a film strip graphic on the left. The text is in white and orange. The main headline reads 'Not all AFMs are created equal' in orange, followed by 'Asylum Research Cypher™ AFMs' in white, and 'There's no other AFM like Cypher' in orange. Below this is the website 'www.AsylumResearch.com/NoOtherAFMLikeIt' in white. In the bottom right corner is the Oxford Instruments logo, which consists of the word 'OXFORD' above 'INSTRUMENTS' inside a square frame, with the tagline 'The Business of Science®' below it.

Not all AFMs are created equal
Asylum Research Cypher™ AFMs
There's no other AFM like Cypher

www.AsylumResearch.com/NoOtherAFMLikeIt

OXFORD
INSTRUMENTS
The Business of Science®

Large-amplitude thermal oscillations in defected, tilted nanocolumns

Bradley C. Hubartt and Jacques G. Amar

Department of Physics and Astronomy, University of Toledo, Toledo, Ohio 43606, USA

(Received 4 September 2014; accepted 3 November 2014; published online 14 November 2014)

We consider the thermomechanical properties of highly defected, tilted copper nanocolumns grown via simulations of glancing angle deposition. The large defect density and compressive strain lead to ultra-low activation energies for plastic deformation via collective shear motion. As a result, the thermal oscillation amplitude is independent of temperature. This leads to a mechanism for large-amplitude thermally induced nanocolumn oscillation, in which the dynamics corresponds to a sequence of correlated activated events. © 2014 AIP Publishing LLC.
[\[http://dx.doi.org/10.1063/1.4901741\]](http://dx.doi.org/10.1063/1.4901741)

Due to their unique mechanical and structural properties,¹ nanocrystalline materials have been the subject of widespread research for several decades. In particular, while for grain sizes above 20–40 nm, the yield strength of bulk polycrystalline metals increases with decreasing grain size,^{2,3} for smaller grain sizes alternative deformation mechanisms^{1,4} such as grain-boundary sliding, migration, and grain rotation play an important role. In addition, the presence of free surfaces has recently been shown to significantly modify the deformation mechanisms of nanoscale structures. For example, a transition^{5,6} in the deformation mechanism of polycrystalline nanocolumns under applied stress—from dislocation-driven to grain-boundary-mediated deformation—has recently been demonstrated at a size of approximately 100 nm. However, while in these works the emphasis was on the response to applied stress, the effects of defects and intrinsic stress on thermomechanical properties have not been studied.

Here, we consider the thermomechanical properties of highly defected, tilted copper nanocolumns. One of the motivations for this work is our desire to gain a fundamental understanding of dynamical effects which control the evolution of the thin-film morphology observed during simulations⁷ of Cu/Cu(100) growth via glancing angle deposition (GLAD) at room temperature. However, another motivation is the development of a fundamental understanding of the role of defects in controlling mechanical properties on the nanoscale. In addition, we note that arrays of nanocolumns may be useful in a variety of applications including advanced data storage,^{8,9} heat transport,¹⁰ and vibrational energy harvesting.^{11–13}

In striking contrast to elastic vibrations, for which the thermal oscillation amplitude increases as the square-root of the temperature, here, we find that both the oscillation amplitude and frequency remain constant over a temperature range of more than two orders of magnitude. As a result, at low temperature, the nanocolumn oscillation amplitude is more than 200 times the prediction of thermal elasticity theory. In addition, we demonstrate that the large defect density and compressive strain, which arise as a result of the nanocolumn formation process,⁷ lead to extremely low activation energies for plastic deformation via collective shear motion. As a result, the thermally induced nanocolumn dynamics corresponds to a series of correlated events. However, in contrast to typical systems in which correlated transitions arise as a

result of the momenta of individual atoms involved in the transition, here the momentum of the entire nanocolumn plays a crucial role.

Our simulations were carried out using the general purpose molecular dynamics (MD) package LAMMPS,¹⁴ along with a highly optimized embedded-atom-method (EAM)¹⁵ potential for Cu which was recently developed by Sheng *et al.*¹⁶ Similar behavior has also been obtained using a slightly different EAM potential.¹⁷ In each case, the nanocolumn as well as the five moving substrate layers beneath it were simulated using a constant energy ensemble with a time-step of 1 fs, while a constant temperature T (ranging from 0.5 K to 300 K) was maintained by damping the three substrate layers below using a Langevin thermostat with a damping time of 10^{-12} s. Two additional fixed layers were included below the moving layers in order to fix the system.

While previously we have studied the dependence of the overall thin-film surface roughness and microstructure on deposition conditions, here our analysis is focused on the dynamical behavior of the “big” and “small” nanocolumns shown in Fig. 1, which were extracted from our previous GLAD simulations⁷ after 15 monolayers (ML) of growth on a Cu(100) substrate with deposition rate 0.3 ML/ns and a deposition angle of 80° at room temperature. In all cases, before collecting the data the extracted system was first minimized, and then equilibrated at the desired temperature for several nanoseconds using Langevin molecular dynamics with damping applied to the middle three substrate layers as described above. To verify that the system was properly equilibrated, we also monitored the temperature of the non-Langevin moving atoms before collecting data.

We note that the somewhat irregular shape of both nanocolumns can be approximately described in terms of three characteristic parameters, the column length L , width w_1 in the tilt plane, and width w_2 in a direction perpendicular to the tilt plane. In particular, for the big (small) column, we have $L = 104 \text{ \AA}$ (88.4 \AA), $w_1 = 20.8 \text{ \AA}$ (26.0 \AA), and $w_2 = 41.6 \text{ \AA}$ (31.2 \AA). As shown in Fig. 1(a) for the big nanocolumn, for both nanocolumns there is a high density of stacking faults of the order of 20%. In addition, both nanocolumns exhibit significant compressive strain which arises as a result of the initial kinetic energy of condensation of depositing atoms near grain boundaries.^{7,18}

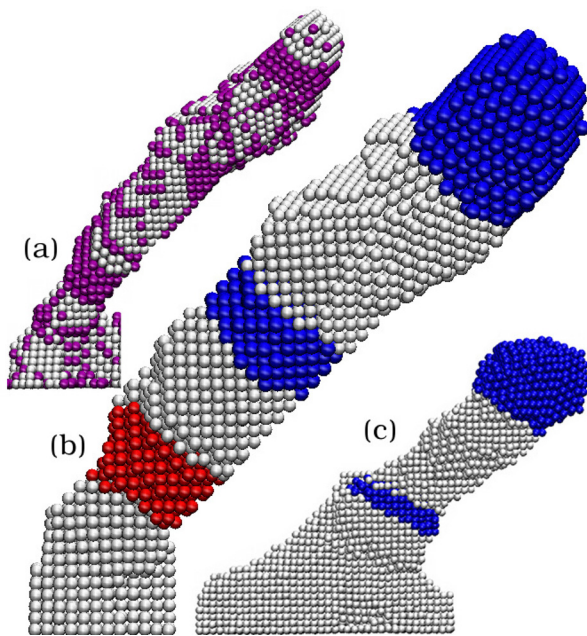


FIG. 1. Snapshots of big and small nanocolumns. (a) Big nanocolumn with surface atoms removed. Defect atoms (mainly stacking faults) are highlighted in purple. (b) Big and (c) small nanocolumns including surface atoms. Blue and red shaded areas correspond to regions with a high density of shear events. Red atoms correspond to atoms with compressive strain larger than 1.5%.

To determine the thermal oscillation amplitude and frequency, we first identified the average position of the tip of each nanocolumn by averaging over a time-period of several nanoseconds after equilibration. The magnitude $|\Delta\mathbf{R}(t)|$ of the displacement of the tip from its average position was then plotted as a function of time and the oscillation amplitude estimated by calculating the average peak to valley difference. Similarly, the oscillation frequency was determined from the average period, corresponding to the average time-interval between successive peaks in $|\Delta\mathbf{R}(t)|$.

Fig. 2 shows typical results for both nanocolumns at $T = 2$ K. As can be seen, the oscillation amplitude for the big nanocolumn ($A_{big} \simeq 1.4$ Å) is significantly larger than that for

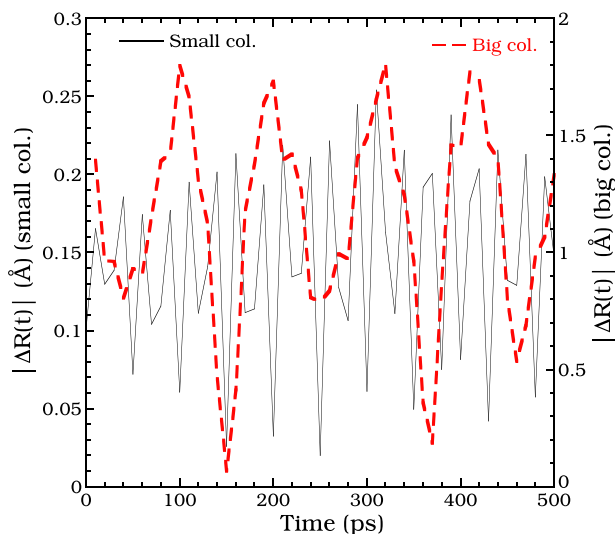


FIG. 2. Displacement of nanocolumn tip as function of time for big and small nanocolumns at 2 K.

the small nanocolumn ($A_{small} \simeq 0.29$ Å), while the oscillation frequency is significantly smaller. In addition, as shown in Fig. 3, examination of the temperature-dependence indicates that for both nanocolumns the oscillation amplitudes are essentially independent of temperature from $T = 0.5$ K to 300 K. This is in striking contrast to the corresponding elasticity theory prediction¹⁹

$$A_{el} = \left[\frac{4k_B T L^3}{E w_1^3 w_2} \right]^{1/2}, \quad (1)$$

(where E is the Young's modulus) which implies a variation of the oscillation amplitude by a factor of 24.5 over this temperature range. As a result, the ratio of the measured amplitude to the elasticity theory prediction for the big (small) nanocolumn (assuming the bulk value of the Young's modulus for Cu) ranges from 7.6 (1.4) at 300 K to 220 (64) at 0.5 K.

While a discrepancy with elasticity theory at a single temperature might be explained by the existence of a reduced Young's modulus which arises as a result of the large defect density, the deviation of the temperature dependence from the elasticity theory prediction strongly suggests that the oscillations are not elastic. This is further confirmed by the fact that, as shown in Fig. 4 for the big nanocolumn at 2 K, the total minimized system energy is not constant, but instead fluctuates with a root-mean-square (r.m.s.) amplitude (0.044 eV). Similar results have also been obtained at 100 K, although at this temperature the r.m.s. minimized energy fluctuation (1.87 eV) is much larger. We note that both of these values are only slightly smaller than those obtained for the r.m.s. fluctuation of the total *non-minimized* system energy, which, as expected, are in good agreement with the classical thermodynamic relation²⁰ $\delta E = (3N)^{1/2} k_B T$, where $N = 20,783$ is the number of moving

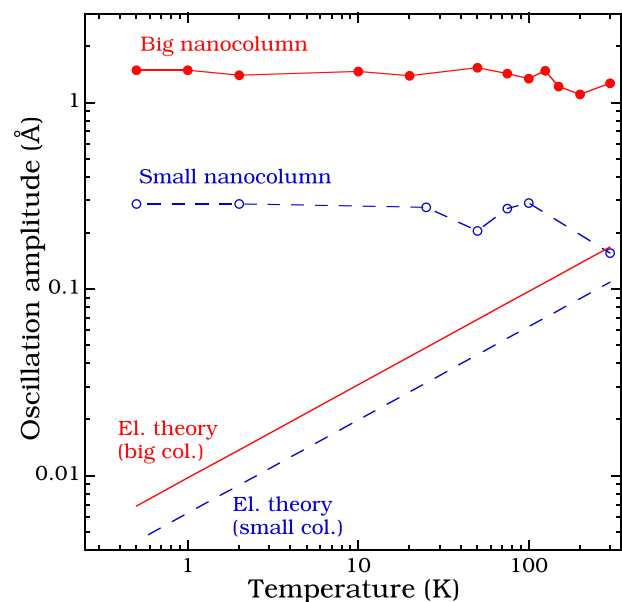


FIG. 3. Comparison between temperature dependence of oscillation amplitudes for big and small nanocolumns with corresponding elasticity theory prediction Eq. (1).

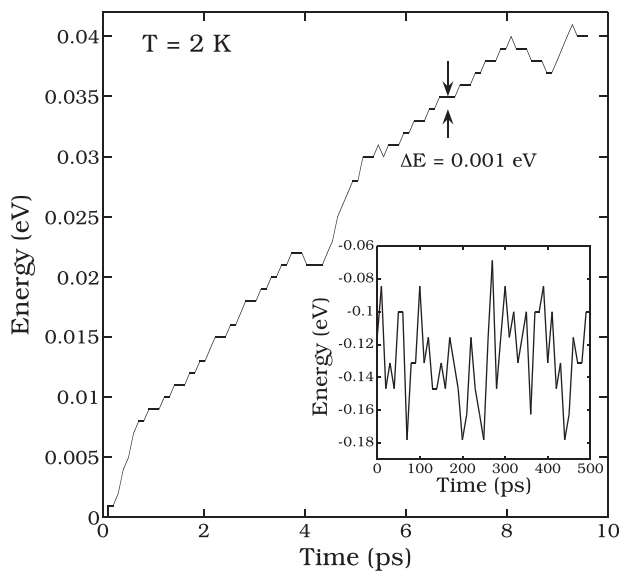


FIG. 4. Evolution of minimized system energy for big nanocolumn over a brief 10 ps interval (data taken every 100 ns). Inset shows corresponding results over a longer 500 ps interval. (Note: zero of energy has been shifted for convenience in both cases.)

atoms in our system. Similar results have also been obtained for the small nanocolumn.

As also indicated in Fig. 4, the trajectory of the big nanocolumn corresponds to a sequence of transitions between minimized states whose energy differences are of the order of 10^{-3} eV or less. This suggests that the corresponding activation barriers are also of the order of 10^{-3} eV or less. We note that these barriers are an order of magnitude smaller than the already very small barriers (of the order of 0.03 eV, see Ref. 21) for stacking fault transitions in Cu. However, they are consistent with the very small barriers observed in Cu for the migration of kinks in screw dislocations^{28,29} (30 μ eV) as well as for the initial motion of jogged edge dislocations (0.004 eV).²⁸

While these results confirm that defects may lead to transitions with very low barriers, strain may also play a significant role,^{23,24} since the average strain in both nanocolumns is compressive while a significant fraction of the atoms experience compressive strains larger than 2%. This is also shown in Fig. 1 for the big nanocolumn, in which the red atoms correspond to a high concentration of defects with compressive strain greater than 1.5%. Thus, we conclude that the combination of compressive strain and a high defect density leads to extremely low barriers for plastic deformation. In contrast, we note that simulations of a perfect (vertical) nanocolumn lead to very small amplitude oscillations in good agreement with elasticity theory.

The extremely small values of the barriers for plastic deformation are also consistent with the observation that the nanocolumn oscillation frequency f does not depend on temperature even at very low temperature (0.5 K). In particular, for the big (small) nanocolumn, we find $f_{big} = 4.5 \pm 0.1$ GHz ($f_{small} = 18.4 \pm 0.3$ GHz) over the temperature range $T = 0.5$ –300 K. Thus, while the temperature independence of the oscillation frequency is also qualitatively consistent²² with elasticity theory, both the variation of the minimized system energy with time as well as the large oscillation amplitude at

low temperature clearly indicate the presence of low-barrier activated events which lead to plastic deformation of the nanocolumn.

Due to the extremely low barriers, it was not possible to use the nudged-elastic-band method^{25,26} to directly determine the energy barriers for individual events. However, an analysis of sequences of minimized configurations at 10 ps intervals indicates the existence of transitions corresponding to the shear displacement of small groups of nearest-neighbor atoms. In each case, the total relative displacement is typically less than $0.6 a_1$, where a_1 is the nearest-neighbor distance. In particular, as shown in Fig. 1, the blue atoms in both the big and small nanocolumns correspond to regions in which shear events occur with relative displacements of nearest-neighbor atoms between $0.4 a_1$ and $0.6 a_1$. In addition, the highly compressed red atoms at the base of the big nanocolumn in Fig. 1 undergo a series of even smaller-scale rearrangements. A detailed examination also indicates that the red and blue regions at the base of the big and small nanocolumns, respectively, act as “hinges” which drive the oscillation. In addition, the blue region in the middle of the big nanocolumn acts as a secondary hinge which enhances the oscillatory behavior.

Fig. 5 shows two typical shear events in the red “hinge” region at the base of the big nanocolumn which correspond to the relative displacement of a cluster of atoms with maximum nearest-neighbor relative displacements of 0.40 Å and 0.42 Å, respectively. We note that these events are somewhat similar to the deformations observed in shear transformation zones^{30–37} of metallic glasses under applied stress. However, the large defect density in this region actually corresponds to a sequence of stacking faults.

While the existence of ultra-low barriers is necessary to explain the large amplitude at low temperature, this alone cannot explain the oscillatory dynamics. For example, a random sequence of low-barrier events would lead to a random walk rather than the observed oscillatory behavior. Accordingly, we expect that correlations play an important role. However, in contrast to typical systems in which correlated transitions arise as a result of the momentum of the atoms involved in the transition,²⁷ here the momentum of the entire nanocolumn plays a crucial role.

In order to examine the impact of correlations on the thermal motion, we have carried out additional simulations at $T = 1$ K, in which a Langevin thermostat was applied to

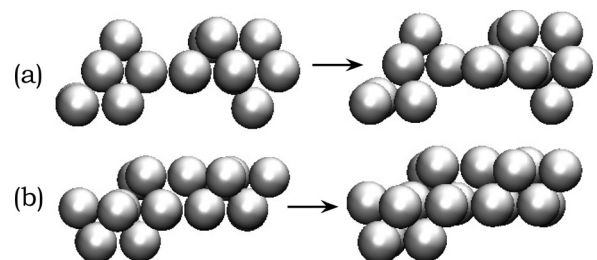


FIG. 5. Typical shear deformations of minimized configurations in the highly compressed “hinge” region (red atoms in Fig. 1(b)) of big nanocolumn at 2 K. Time interval between snapshots is 10 ps. In (a), the largest relative displacement is 0.42 Å, while in (b), the largest relative displacement is 0.4 Å.

the atoms in the nanocolumn as well as the substrate. For a damping time of 1 ps (comparable to an atomic oscillation period), we find that the nanocolumn oscillation amplitude is decreased by a factor of 70, while the corresponding frequency is increased by a factor of 3. As a result, the oscillation amplitude (0.03 Å) is much closer to the elasticity theory prediction (0.01 Å) assuming the bulk modulus of Cu, while the frequency is in good agreement with the corresponding prediction. Interestingly, we find that in this case the fluctuations of the minimized energy are approximately the same as was found in the absence of Langevin damping. Thus, while the Langevin damping does not eliminate the low-barrier shear events, due to the suppression of correlations the oscillation amplitude is significantly reduced. In contrast, for a much longer damping time of 6.9 ns (31 times the undamped oscillation period) the oscillation amplitude is only reduced by a factor of two, while the frequency is unaffected. These results clearly demonstrate the importance of correlations which are suppressed even in the presence of a small random Langevin force.

In conclusion, we have demonstrated the existence of large amplitude temperature-independent oscillations in nanocolumns grown via simulations of glancing angle deposition. In particular, our results indicate that the large defect density and compressive strain lead to ultra-low activation energies for plastic deformation via collective shear motion. This leads to large amplitude temperature-independent oscillations, in which the dynamics consists of a sequence of correlated plastic deformations driven by the motion of the entire nanocolumn. In general, we expect that the existence of significant compressive strain as well as a large defect density may lead to similar behavior in more complex nanostructures.

We would like to acknowledge useful discussions with Robin L. Blumberg Selinger and Art Voter. This research was supported by NSF Grant Nos. DMR-0907399 and DMR-1410840 as well as a grant of computer time from the Ohio Supercomputer Center.

¹M. A. Meyers, A. Mishra, and D. J. Benson, *Prog. Mater. Sci.* **51**, 427 (2006).

²E. O. Hall, *Proc. Phys. Soc. London B* **64**, 747 (1951).

³N. J. Petch, *J. Iron Steel Inst.* **174**, 25 (1953).

⁴X. Li, W. Hu, S. Xiao, and W.-Q. Huang, *Physica E* **40**, 3030 (2008).

⁵D. Jang and J. R. Greer, *Scr. Mater.* **64**, 77 (2011).

- ⁶S. V. Bobylev and I. A. Ovid'ko, *Phys. Rev. Lett.* **109**, 175501 (2012).
- ⁷B. Hubartt, X. Liu, and J. G. Amar, *J. Appl. Phys.* **114**, 083517 (2013).
- ⁸A. K. Kar, P. Morrow, X.-T. Tang, T. C. Parker, H. Li, J.-Y. Dai, M. Shima, and G.-C. Wang, *Nanotechnology* **18**, 295702 (2007).
- ⁹H. Su, A. Natarajarathinam, and S. Gupta, *J. Appl. Phys.* **113**, 203901 (2013).
- ¹⁰D. V. Averin and J. P. Pekola, *Phys. Rev. Lett.* **104**, 220601 (2010).
- ¹¹S. P. Beeby, M. J. Tudor, and N. M. White, *Meas. Sci. Technol.* **17**, R175 (2006).
- ¹²F. Cottone, H. Vocca, and L. Gammaitoni, *Phys. Rev. Lett.* **102**, 080601 (2009).
- ¹³C. Kim, M. Prada, G. Platero, and R. H. Blick, *Phys. Rev. Lett.* **111**, 197202 (2013).
- ¹⁴S. Plimpton, *J. Comput. Phys.* **117**, 1 (1995), see <http://lammps.sandia.gov>.
- ¹⁵M. S. Daw and M. I. Baskes, *Phys. Rev. B* **29**, 6443 (1984).
- ¹⁶H. W. Sheng, M. J. Kramer, A. Cadien, T. Fujita, and M. W. Chen, *Phys. Rev. B* **83**, 134118 (2011).
- ¹⁷Y. Mishin, M. J. Mehl, D. A. Papaconstantopoulos, A. F. Voter, and J. D. Kress, *Phys. Rev. B* **63**, 224106 (2001).
- ¹⁸C.-W. Pao, S. M. Foiles, E. B. Webb, D. J. Srolovitz, and J. A. Floro, *Phys. Rev. Lett.* **99**, 036102 (2007).
- ¹⁹H.-J. Butt and M. Jaschke, *Nanotechnology* **6**, 1 (1995).
- ²⁰L. E. Reichl, *A Modern Course in Statistical Physics*, 3rd ed. (Wiley-VCH Verlag, 2009).
- ²¹M.-C. Marinica, C. Barreteau, M.-C. Desjonquères, and D. Spanjaard, *Phys. Rev. B* **70**, 075415 (2004).
- ²²Assuming bulk values of the Young's modulus E and density ρ for Cu, the classical elasticity theory prediction for the vibration frequency²⁰ $f_{el} = 0.161 \frac{\nu_s}{L^2} \left(\frac{E}{\rho}\right)^{1/2}$ leads to a predicted vibrational frequency $f_{el}^{small} \simeq 19.7$ GHz for the small nanocolumn which is in surprisingly good agreement with our simulations. In contrast, the corresponding calculated frequency for the big nanocolumn ($f_{el}^{big} \simeq 11.4$ GHz) is almost 3 times larger than obtained in our simulations.
- ²³C. Ratsch, A. P. Seitsonen, and M. Scheffler, *Phys. Rev. B* **55**, 6750 (1997).
- ²⁴Y. Shim and J. G. Amar, *Phys. Rev. Lett.* **108**, 076102 (2012).
- ²⁵H. Jónsson, G. Mills, and K. W. Jacobsen, in *Classical and Quantum Dynamics in Condensed Phase Simulations*, edited by B. J. Berne, G. Cicciotti, and D. F. Coker (World Scientific, Singapore, 1998), p. 385.
- ²⁶G. Henkelman, B. P. Uberuaga, and H. Jónsson, *J. Chem. Phys.* **113**, 9901 (2000).
- ²⁷G. Antczak and G. Ehrlich, *Surf. Sci. Rep.* **62**, 39 (2007).
- ²⁸T. Vegge and K. W. Jacobsen, *J. Phys.: Condens. Matter* **14**, 2929 (2002).
- ²⁹G. Schottky, *Phys. Status Solidi A* **5**, 697 (1964).
- ³⁰M. L. Falk and J. S. Langer, *Phys. Rev. E* **57**, 7192 (1998).
- ³¹F. Spaepen, *Acta Metall.* **25**, 407 (1977).
- ³²A. Argon, *Acta Metall.* **27**, 47 (1979).
- ³³A. Argon and H. Kuo, *Mater. Sci. Eng.* **39**, 101 (1979).
- ³⁴A. Argon and L. Shi, *Acta Metall.* **31**, 499 (1983).
- ³⁵V. Khonik and A. Kosilov, *J. Non-Cryst. Solids* **170**, 270 (1994).
- ³⁶M. L. Falk, J. S. Langer, and L. Pechenik, *Phys. Rev. E* **70**, 011507 (2004).
- ³⁷J. S. Langer and L. Pechenik, *Phys. Rev. E* **68**, 061507 (2003).